Crack tip fields and mixed mode fracture behaviour of progressively drawn pearlitic steel

J. Toribio, B. González, J.C. Matos
University of Salamanca
toribio@usal.es

ABSTRACT. This paper deals with the influence of the cold drawing process on the fracture behaviour of pearlitic steels. To this end, fracture tests under axial loading were performed on steel wires with different drawing degree (from a hot rolled bar to a commercial prestressing steel wire), transversely pre-cracked by fatigue, analyzing in detail the changes in fracture micromechanisms. The deflection angles of the fracture path were measured by longitudinal metallographic sections and the characteristic parameters of the load-displacement plot were related to different fracture events. Results allowed a calculation of critical stress intensity factors for different fracture angles and drawing degrees, thus evaluating the strength anisotropy and obtaining a sort of directional toughness.

KEYWORDS. Progressively drawn pearlitic steel; Strength anisotropy; Crack path deflection; Mixed mode fracture; Directional toughness.

INTRODUCTION

The micro-mechanisms taking place during the fracture process of metals and alloys, as well as the fracture toughness, change with the temperature, the loading rate, and the cold work [1-3]. In the particular case of pearlitic steel used to produce high-strength cold-drawn prestressing wires, the cold drawing process affects the phenomenon of the fracture, so that the most heavily drawn steels (undergoing severe plastic deformation) exhibit strength anisotropy, and a change in the crack propagation direction, which approaches the wire axis or drawing direction [4]. This leads to the calculation of two values of the angular fracture toughness, one in the radial direction and the other in the axial one, the first being much greater than the second for steels with severe plastic deformation [5-7]. In wires with axisymmetric notches, the degree of the fracture anisotropy also depends on the notch geometry [8].

The fracture surface of pearlitic steel presents a change in the fracture mechanism as the wire is drawn [6]. In the hot rolled wire the fracture is produced through cleavage, while in the early stages of cold drawing there appears fracture caused by growth and coalescence of microvoid and then cleavage. On the other hand, the heavily drawn steels exhibit, after the propagation of microvoids in mode I, a step at about 90° followed by a mixed propagation of microvoids and cleavage [4]. The fracture behaviour of pearlitic steel mainly depends on the size of the prior austenite grain [9-11]: the smaller the size of the grain, the greater the fracture toughness. If the pearlitic steel is cold drawn, then the pearlite colony, rather than the prior austenite grain, is the critical fracture unit determining the size of the cleavage facet [12].

This paper deals with the anisotropic fracture behaviour of eutectoid pearlitic steel wires with different degree of cold drawing (distinct level of strain hardening and diverse microstructural arrangements) exhibiting strength anisotropy. The analysis is focused on the crack path deflection angle and the directional toughness.

EXPERIMENTAL PROCEDURE

A progressively drawn pearlitic steel, eutectoid chemical composition (Tab. 1), was used in this work: from the hot-rolled bar (not cold drawn at all) to the cold drawn wire (obtained after seven cold drawing steps and a stress-relieving treatment), as well as the intermediate steps. The code used to designate the steel consists of the letter B followed by a digit indicating the number of drawing steps applied to each one.

%C	%Mn	%Si	%P	%Cr	%V
0.789	0.681	0.210	0.010	0.218	0.061

Table 1: Chemical composition (wt %) of the steels.

The degree of cold drawing is characterized by means of the cumulative plastic strain ε^{p} as a function of the diameter reduction according to the following expression,

$$\varepsilon^{\mathrm{p}} = \ln \frac{D_0}{D_i} \qquad (1)$$

where D_i is the diameter of the wire after i drawing steps and D_0 that corresponding to the initial steel wire.

The stress-strain curves (Fig. 1) and the conventional mechanical properties were obtained by means of a standard tension test. The cold drawing process does not modify the Young's modulus E (~200 GPa), and produces a clear improvement of material strength in the form of increase of both yield strength σ_Y and ultimate tensile strength (UTS) σ_R (Fig. 2).
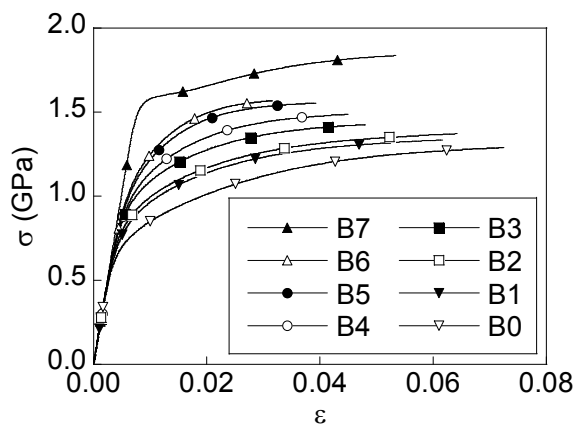

Figure 1: Stress-strain curves σ-ε (standard tension tests).
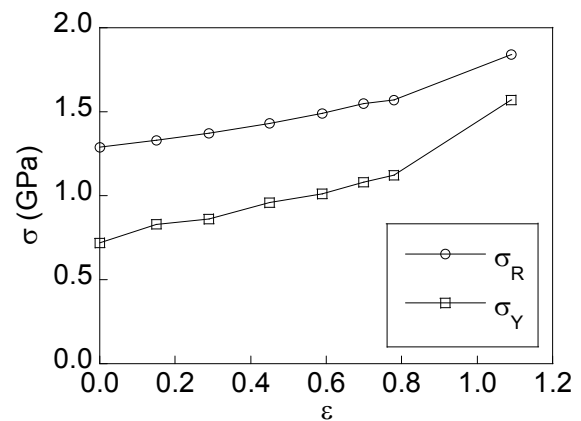

Figure 2: Mechanical properties as a function of the strain hardening level.

To evaluate the fracture toughness, a standard measurement procedure could not be applied because of the scarcity of the material (supplied in either bar or wire form with different diameters). The method applied in this paper is based in the calculation (from experimental measurements) of a critical stress intensity factor (SIF) and the use of a local fracture criterion, as explained elsewhere [13].

To perform the fracture tests, samples of 300 mm were taken from the wires, with diameters of 12 mm in the hot rolled bar and 7 mm in the cold drawn wire. Samples were precracked by means of axial tensile fatigue with a sinusoidal wave (at a frequency of 10 Hz and R-ratio equal to 0) under load control and decreasing loading steps. The maximum value of the stress intensity factor at the end of precracking was 25-30 MPam$^{1/2}$. After this fatigue precracking, specimens were subjected to monotonic tensile loading under displacement control up to fracture, the crosshead speed being 3 mm/min. An extensometer was placed in front of the crack mouth (symmetrically in relation to the crack faces), so that both the load applied on the sample (F) and the relative displacement by the extensometer (u) were recorded to plot the load-displacement curve F-u.

EXPERIMENTAL RESULTS

Microstructural analysis

Figure 3 shows the microstructure of hot rolled bar and prestressing steel wire, longitudinal section, where the horizontal size of the micrograph corresponds to the radial direction and the vertical size is associated with the axial direction in the longitudinal cut. The drawing process produces important microstructural changes in the steel at the two basic microstructural levels of pearlitic colonies and lamellae. The colonies become progressively enlarged and oriented in axial direction with cold drawing. With regard to the lamellae, they are also axially oriented after drawing and, at the same time, the pearlite interlamellar spacing decreases with the level of cumulative plastic strain. Therefore, the microstructure becomes progressively packed and oriented with cold drawing.
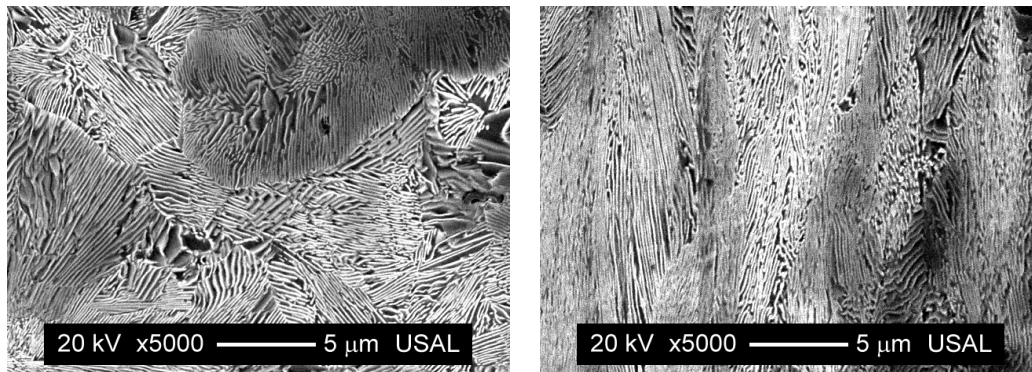

Figure 3: Microstructure, longitudinal section, B0 (left) and B7 (right).

Fracture surface

Fig. 4 shows the fracture surface for the different steels, where the fatigue surface, starting from a small mechanical cut (on the left side of the photographs), appears with a semi-elliptical final front from which the fracture initiates. Macroscopically, the fracture surfaces of the slightly drawn steels propagate perpendicularly to the applied stress, following the fatigue crack. On the contrary, in heavily drawn steels, the fracture is very anisotropic, with abundant deflections and longitudinal cracking.

Symmetrical longitudinal cuts were made in the fracture-tested specimens, they were photographed (Fig. 5), and the fracture angle was measured. In these photographs the fatigue growth is shown on the left, with a flatter profile, in addition to the fracture appearing after such a fatigue growth. As the plastic deformation increases with the number of drawing steps, so does the roughness of the fracture surface, as well as the fracture angle θ (in relation to the cross section of the wire), which implies the occurrence of a fracture in mixed mode. Furthermore, in heavily-drawn steels, the existence of a step oriented with an angle of 90º (in relation to the cross section of the wire) can be observed at the beginning of the fracture event.
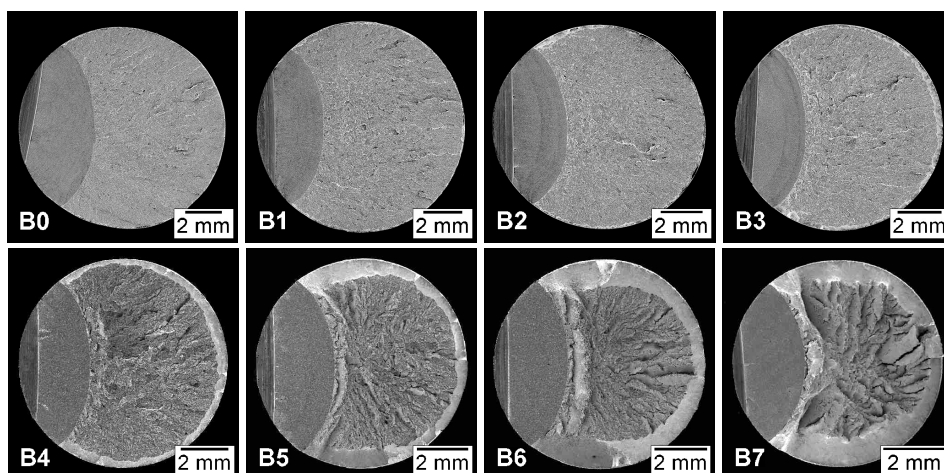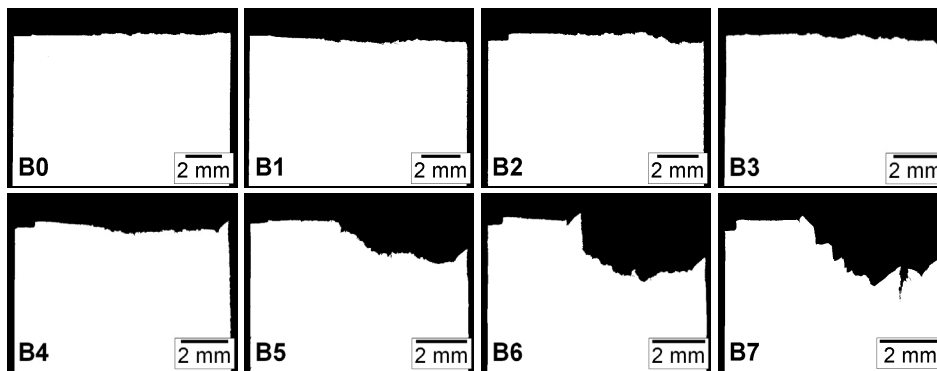

Figure 4: Fracture surfaces, B0 to B7.

Figure 5: Longitudinal section of the fracture, B0 to B7.

Crack fronts are characterized by a semi-elliptical geometry centred on the surface of the wire. In slightly-drawn steels, a micro-void coalescence (MVC) zone appears at the fracture surface after fatigue crack, with an extension of a few tenths of a micron, whose surface increases with the cold-drawing process. Then the fracture propagates by cleavage and ends with a small external ring of MVC. The initial MVC zone is not taken into account in the calculations (due to its small size); instead of it, the crack front used in the calculations is that created by fatigue. It is modelled as a part of an ellipse of semiaxes a_f and b_f, with a_f coincident with the crack depth.

In heavily drawn steels, the main fracture micro-mechanisms are MVC and vertical walls consisting of elongated cleavage. Such walls appear surrounding the fatigue crack in the form of abundant secondary radial cracking, and their sizes increase in extension with cold drawing. The final external ring of MVC has a greater surface than in slightly drawn steels. The crack growth area prior to the first propagation step (oriented with an angle of 90°) has a size on the order of hundreds of microns, and is taken into account in the calculations, resulting in the appearance of two critical crack sizes during the fracture: the fatigue crack (with semiaxes a_f and b_f), and the crack existing at the time of growth of the afore-said 90° crack propagation step (with semiaxes a_e and b_e).

Load-displacement curve

The records obtained for the load-displacement curve *F-u* are different for slightly- and heavily-drawn steels (Fig. 6). Both have an initial linear zone that becomes a curve, with this curvature being generally greater as the drawing process increases, although it could also depend on other factors. The curves were characterized from two parameters: the load at the end of the linear behaviour portion of the curve (F_e) and the maximum load (F_{max}). In heavily drawn steels, a characteristic load (F_Y) also appears that can be associated with a micro-tearing phenomenon called *pop-in* [14], which is accompanied by a characteristic tearing noise. By performing interrupted tests [15], it has been observed that the phenomenon of *pop-in* is physically associated with the occurrence of vertical cracking.
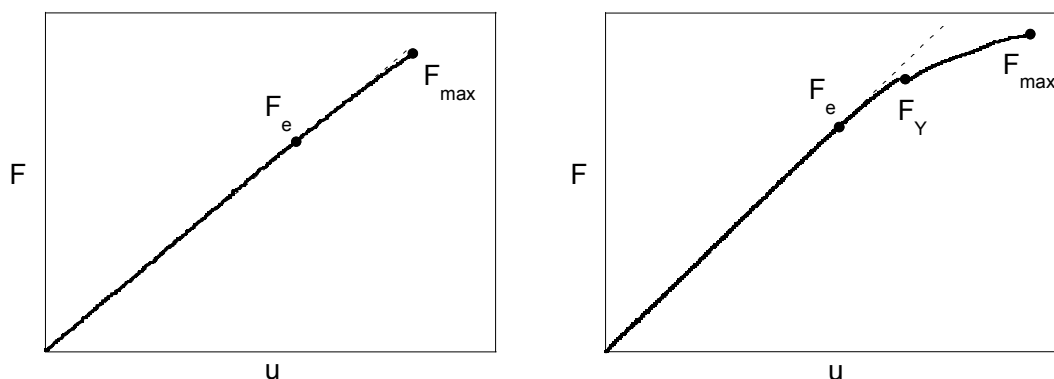

Figure 6: Load-displacement curve, B0 (left) and B7 (right).

Fracture toughness

The value of the critical SIF, obtained for cracked cylindrical specimens, is the fracture toughness of the material, being independent of the wire's diameter and of the crack size. Once the fracture tests were carried out, the critical SIF

corresponding to the macroscopic angle of the fracture surface (K_{C0}) was calculated, as well as the critical SIF associated with the *pop-in* phenomenon ($K_{C90°}$) for those steels where a vertical step existed. To calculate these characteristic values, the maximum SIF was considered over practically the whole crack front in which plane strain conditions occur (the points at the wire surface were not taken into account in the calculations of the characteristic SIF).

On the basis of previous research [16], the dimensionless SIF Y used in the computations is that proposed by Shin and Cai [17] in the form of a three-parameter expression as a function of the relative crack depth a/D, the crack aspect ratio a/b and the position along of the crack front x/h:

$$K_{I0°} = K_{I0°}(F, a, b) = Y\left(\frac{a}{D}, \frac{a}{b}, \frac{x}{h}\right)\sigma\sqrt{\pi a} \tag{2}$$

To obtain the SIF of a secondary crack with angle θ from the main one (Fig. 7), it has been considered that the local SIFs at the tip of a secondary crack (k_1^*, k_2^*) are related with the global SIFs from the main crack (K_I, K_{II}) for the case in which the secondary crack length tends to zero [18]. The expression of the local SIFs, for the crack tip in deflection, is given by:

$$\begin{pmatrix} k_1^* \\ k_2^* \end{pmatrix} = \begin{pmatrix} K_{11} & K_{12} \\ K_{21} & K_{22} \end{pmatrix}\begin{pmatrix} K_I \\ K_{II} \end{pmatrix} \tag{3}$$

where the coefficients K_{ij} only depend on the value of the deflection angle θ. For the calculations, the coefficients obtained by Amestoy [18] were used, fitted to third-order polynomial expressions with high regression coefficients.
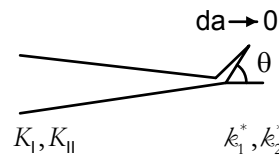

Figure 7: Crack tip deflection.

The energy release rate value satisfies the following expression [18, 19]:

$$G = \frac{(k_1^{*2} + k_2^{*2})}{E'} \tag{4}$$

where $E' = E/(1-\nu^2)$ in plane strain and $E' = E$ in plane stress.

In the matter of the materials that exhibit an anisotropic fracture behaviour, the fracture specific energy depends on the angle of propagation, θ, with respect to the crack plane (contained in the wire cross section). The directional energy release rate, $G(\theta)$, can be related to the energy release rate at 0°, $G(0°)$, and similarly their critical values:

$$G(\theta) = (K_{11}^2 + K_{21}^2)G(0°) \tag{5}$$

For the slightly drawn steels, Eq. 6 allows the calculation of the directional fracture toughness, keeping in mind the maximum load and the size of the fatigue crack:

$$K_{C\theta} = \sqrt{K_{11}^2 + K_{21}^2}\, K_{I0°}(F_{max}, a_f, b_f) \tag{6}$$

In heavily drawn steels, the critical SIF was calculated in mode I at 90°, from the *pop-in* load. In the fracture step, corresponding to the vertical cleavage burst (Fig. 8), the relationship between the energy release rate in the axial direction (for the 90° angle) and in the radial direction (for 0°) [18] permits the calculation of the critical SIF at 90°.
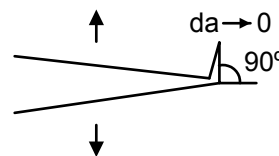

Figure 8: Crack tip deflection towards 90°.

The critical SIF at 90° can be obtained as follows [6, 7]:

$$K_{C90°} = \sqrt{0.2615} K_{I0°}(F_Y, a_e, b_e) \tag{7}$$

In the crack propagation from the vertical cleavage wall, which appears in the heavily drawn steels, the energy release rate for crack growth in the fracture plane oriented with an angle θ can be obtained after simplification by neglecting the vertical deflection length (Fig. 9).
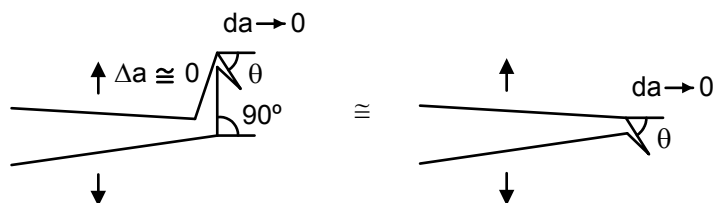

Figure 9: Crack tip deflection towards θ.

Thus, the critical SIF at θ can be calculated as:

$$K_{C\theta} = \sqrt{K_{11}^2 + K_{21}^2} K_{I0°}(F_{max}, a_e, b_e) \tag{8}$$

Fig. 10 shows the results related to the critical SIF in mode I for the fracture angle θ of each drawing step, as well as those linked with the critical SIF in mode I for the fracture angle 90° in those steels where the anisotropy takes place in the form of vertical cracking. Both directional toughness values increase with the drawing process, but the increase of critical SIF associated with the θ angle is much more pronounced than that related to the 90° angle, the former reaching values as high as 110 MPam$^{1/2}$. To assure the adequacy of using the SIF as the key parameter governing the fracture process (through its critical value at the fracture instant), an estimation was performed of the plastic zone size in the vicinity of the crack tip at such a moment in the cases in which the fracture process develops in mode I (precisely the most brittle fracture events) or with a negligible component of mode II. In those cases crack tip plasticity is confined in the near tip region, because the plastic zone size never exceeds 10% of the uncracked ligament, thereby indicating that the critical SIF is adequate as a key parameter governing fracture. For heavily drawn steels the situation is not so clear, because mixed mode propagation appears and thus the plastic zone size cannot be easily estimated. However, even in these more ductile cases the SIF can be considered as an adequate parameter due to the global constraint (triaxiality) provided by the plane strain stress state in the inner points of the crack front.
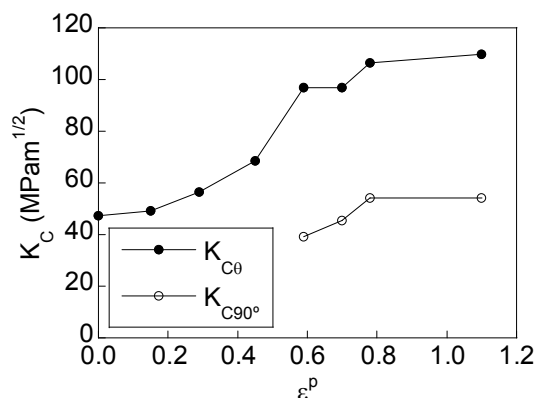

Figure 10: Fracture toughness, $K_{C\theta}$ and $K_{C90°}$.

DISCUSSION

Cold drawing is an effective process for increasing the strength of pearlitic steel, resulting in a considerable improvement in the matter of fracture behaviour (this is very important from the practical engineering viewpoint) while at the same time a strong anisotropy appears during fracture, it being related to microstructural anisotropy produced by plastic deformation as a consequence of cold drawing. Similar results were obtained in a fully pearlitic rail steel subjected to large shear strains by equal channel angular pressing (ECAP) [3] and by high-pressure torsion (HPT) [20].

With regard to the relationship between the macroscopic fracture behaviour of the wires and the microstructure of the progressively drawn pearlitic steels, Fig. 11 represents the fracture angle θ (macroscopic) and the pearlite lamellae angle θ_m (microscopic), both measured in relation to the cross section of the wire, and plotted as a function of the cumulative plastic strain (a measure of the strain hardening level or cold drawing degree in the steel wires). It is seen in Fig. 11 shows how both macro- and micro-angles increase with plastic deformation, thereby showing how the cumulative plastic strain (and its associated microstructural orientation inside the material) affects the fracture performance of the wires in the form of strength anisotropy, crack path deflection and mixed mode propagation.
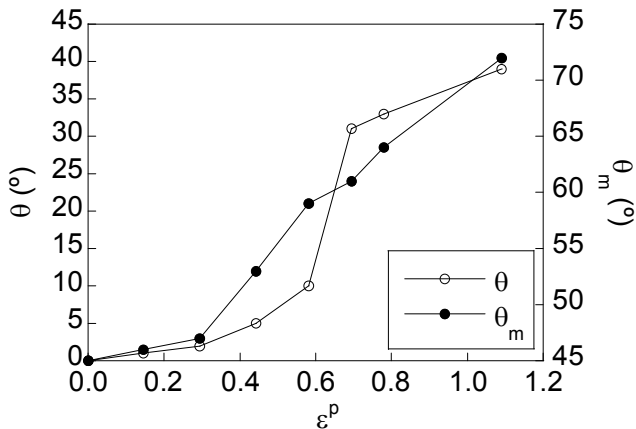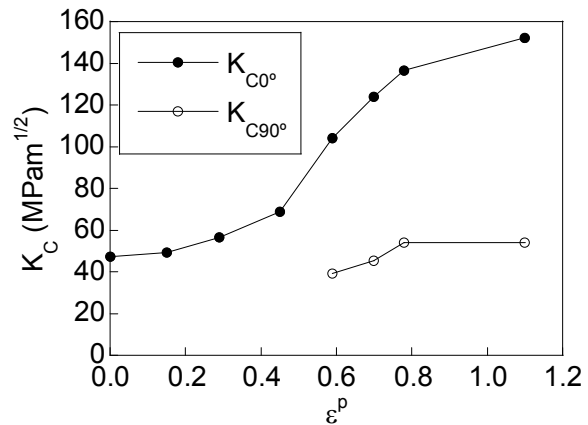

Figure 11: Fracture angle.

Figure 12: Fracture toughness, $K_{C0°}$ and $K_{C90°}$.

The calculation of the critical SIF in mode I at 0° was carried out in a linear way when values were available for both angles. When only the critical SIF for an angle different from 0° was available, the slope was not considered, because it was small. Results show that the steel becomes more anisotropic in its fracture behaviour as the number of wire drawing steps increases (Fig. 12). Furthermore, $K_{C0°}$ markedly increases with plastic deformation, tripling itself, while $K_{C90°}$ only slightly increases.

For high deformations, $K_{C90°}$ is significantly lower than $K_{C0°}$, which explains the presence of vertical cleavage walls on the fracture surfaces (and specially the first propagation step oriented 90° in relation to transverse section). This phenomenon can be related to the existence of a rounded crack tip causing a cleavage stress in the horizontal direction, tending to open a vertical cleavage crack [15], in addition to the microstructural anisotropy caused by the wire drawing itself.

CONCLUSIONS

Cold drawing in pearlitic steel induces strength anisotropy associated with a deflection angle in the crack path, changing from being transversal to the wire (in the non-drawn steel) to producing crack deflection with an ever increasing angle as the degree of cold drawing increases during manufacture.
The directional toughness (or directional critical stress intensity factor, SIF) depends on the deflection angle (macroscopic) of the fracture crack path, such an angle being in turn a function of the microstructural orientation angle of the pearlite lamellae (which tend to be oriented in the wire axis or cold drawing direction).
The cold drawing process improves the fracture behavior in mode I for a 0° angle in pearlitic steel (by increasing the fracture toughness and improving the engineering performance), but it induces a marked anisotropy in its fracture behaviour (strength anisotropy, greater with increasing amount of plastic deformation after drawing) due to the strong microstructural anisotropy.

ACKNOWLEDGEMENTS

REFERENCES

[1] Juhas, M.C., Bernstein, I.M., Effect of prestrain on the mechanical properties of eutectoid steel, Metall. Trans. A, 14 (1983) 1379–1388.

[2] Yu, S.R., Yan, Z.G., Cao, R., Chen, J.H., On the change of fracture mechanism with test temperature, Eng. Fract. Mech., 73 (2006) 331–347.

[3] Wetscher, F., Stock, R., Pippan, R., Changes in the mechanical properties of a pearlitic steel due to large shear deformation, Mater. Sci. Eng. A, 445–446 (2007) 237–243.

[4] Toribio, J., Toledano, M., Fatigue and fracture performance of cold drawn wires for prestressed concrete, Constr. Build. Mater., 14 (2000) 47–53.

[5] Astiz, M.A., Valiente, A., Elices, M., Bui, H.D., Anisotropic fracture behaviour of prestressing steels, in: L.O. Faria (ed.), Life Assessment of Dynamically Loaded Materials and Structures - ECF5, EMAS, Portugal, (1985) 385–396.

[6] Toribio, J., Valiente, A., Approximate evaluation of directional toughness in heavily drawn pearlitic steels, Mater. Lett., 58 (2004) 3514–3517.

[7] Toribio, J., Valiente, A., Failure analysis of cold drawn eutectoid steel wires for prestressed concrete, Eng. Fail. Anal., 13 (2006) 301–311.

[8] Toribio, J., Ayaso, F.J., Fracture performance of progressively drawn pearlitic steel under triaxial stress states, Mater. Sci., 37 (2001) 707–717.

[9] Alexander, D.J., Bernstein, I.M., The cleavage plane of pearlite, Metall. Trans. A, 13 (1982) 1865–1868.

[10] Park, Y.J., Bernstein, I.M., The process of crack initiation and effective grain size for cleavage fracture in pearlitic eutectoid steel, Metall. Trans. A, 10 (1979) 1653–1664.

[11] Fernández-Vicente, A., Carsí, M., Peñalba, F., Taleff, E., Ruano, O.A., Toughness dependence on the microstructural parameters for an ultrahigh carbon steel (1.3 wt.% C), Mater. Sci. Eng. A, 335 (2002) 175–185.

[12] Toribio, J., Ayaso, F.J., Anisotropic fracture behaviour of cold drawn steel: a materials science approach, Mater. Sci. Eng. A, 343 (2003) 265–272.

[13] Toribio, J., A fracture criterion for high-strength steel cracked bars, Struct. Eng. Mech., 14 (2002) 209–222.

[14] Singh, U.P., Banerjee, S., On the origin of pop-in crack extension, Acta Metall. Mater., 39 (1991) 1073–1084.

[15] Toribio, J., González, B., Matos, J.C., Cleavage stress required to produce fracture path deflection in cold-drawn prestressing steel wires, Int. J. Fract., 144 (2007) 189–196.

[16] Toribio, J., Álvarez, N., González, B., Matos, J.C., A critical review of stress intensity factor solutions for surface cracks in round bars subjected to tension loading, Eng. Fail. Anal., 16 (2009) 794–809.

[17] Shin, C.S., Cai, C.Q., Experimental and finite element analyses on stress intensity factors of an elliptical surface crack in a circular shaft under tension and bending, Int. J. Fract., 129 (2004) 239–264.

[18] Amestoy, M., Bui, H.D., Dang-Van, K., Analytic asymptotic solution of the kinked crack problem, in: D. Francois (ed.), Advances in Fracture Research - ECF5, Pergamon Press, France, (1981) 107–113.

[19] Wu, C.H., Fracture under combined loads by maximum-energy-release-rate criterion, J. App. Mech., 45 (1978) 553–558.

[20] Hohenwarter, A., Taylor, A., Stock, R., Pippan, R., Effect of large shear deformations on the fracture behavior of a fully pearlitic steel, Metall. Mater. Trans. A, 42 (2011) 1609–1618.